A High-Lift Building Block Flow: Turbulent Boundary Layer Relaminarization A Final Report

Corey Bourassa, Graduate Research Assistant
Flint O. Thomas, Professor
Robert C. Nelson, Professor

Department of Aerospace & Mechanical Engineering
University of Notre Dame
Notre Dame, IN 46556

Funds for the support of this study have been provided by NASA Dryden Flight Research Center under Grant Number NAG 4-123

May 9, 2000

Abstract

Experimental evidence exists which suggests turbulent boundary layer relaminarization may play an important role in the inverse Reynolds number effect in high-lift systems. An experimental investigation of turbulent boundary layer relaminarization has been undertaken at the University of Notre Dame's Hessert Center for Aerospace Research in cooperation with NASA Dryden Flight Research Center. A wind tunnel facility has been constructed at the Hessert Center and relaminarization achieved. Preliminary evidence suggests the current predictive tools available are inadequate at determining the onset of relaminarization. In addition, an in-flight relaminarization experiment for the NASA Dryden FTF-II has been designed to explore relaminarization at Mach and Reynolds numbers more typical of commercial high-lift systems.

Contents

List of Figures

List of Tables

Nomenclature

c	FTF-II airfoil chord
c_f	skin friction coefficient
$C_{L_{max}}$	maximum aircraft coefficient of lift
C_p	coefficient of pressure
h	height of wind tunnel test section
H	shape factor
K	acceleration parameter, turbulent kinetic energy
L	streamwise length of converging wind tunnel test section, length of FTF-II
M_∞	freestream Mach number
P	pressure
R	correlation parameter, radius of FTF-II leading-edge
Re	Reynolds number
t	FTF-II airfoil thickness
T_B	mean time between burst-sweep events
u	velocity in the streamwise direction
$-\overline{uv}$	Reynolds stress
u_τ	friction velocity
U_∞	freestream velocity
v	velocity in the wall normal direction
x	streamwise distance
y	wall normal distance

Greek Symbols

δ	boundary layer thickness
δ^*	displacement thickness
Λ	integral length scale
ν	kinematic viscosity

τ	wall shear stress
θ	momentum thickness

Subscripts

o	indicates initial streamwise location of wind tunnel contraction

Superscripts

$+$	indicates inner-variable scaling (unless otherwise indicated)

1 Introduction

In a 1996 report entitled "Key Topics for High-Lift Research: A Joint Wind Tunnel/Flight Test Approach"[1] supported by NASA Dryden, Thomas et al. proposed a joint experimental investigation of a to-be-determined high-lift building block flow utilizing the University of Notre Dame's Hessert Center's low speed wind tunnels and NASA Dryden's Flight Test Fixture (FTF-II). Following the recommendation outlined in the report, an internal study conducted by the authors was initiated to determine which high-lift building block flow would be investigated. Results from an extensive literature search and high-lift research conducted at the University of Notre Dame, led to the selection of turbulent boundary layer relaminarization as the most suitable high-lift building block flow for the joint wind tunnel/flight test investigation.

1.1 Relaminarization & High-Lift Systems

In a high-lift system, there is evidence to show that relaminarization of the main element boundary layer may have a profound effect on the global aerodynamic behavior of the system. If one examines the effect of Reynolds number on $C_{L_{max}}$ of a high-lift system, experience dictates that for increasing Reynolds number $C_{L_{max}}$ would increase. In fact, this is not always the case as can be seen in Figure 1, which demonstrates an example of $C_{L_{max}}$ behavior for a high-lift system. As one can see, the low Reynolds number region is approximately linear, but as Reynolds number increases $C_{L_{max}}$ decreases dramatically until at even larger Reynolds number it begins to increase again. Although it is not illustrated in Figure 1, at even greater Reynolds numbers flight test experiments have shown that $C_{L_{max}}$ can drop off again. This phenomena is referred to as the "Inverse Reynolds Number Effect" and its cause is unknown. If one was interested in high Reynolds number behavior, as is often the case for flight aircraft, merely extrapolating from low Reynolds number data typical of wind tunnel tests would be insufficient.

Flight test experiments on leading edge transition and relaminarization conducted by van Dam et al.[2] using the NASA Transport Systems Research Vehicle, a Boeing 737-100, has provided tantalizing evidence, but not proof, that relaminarization may be responsible for the inverse Reynolds number effect that can occur at high Reynolds numbers. Relaminarization in high-lift systems may occur as the turbulent boundary layer proceeds from the attachment location, under the leading edge, around the nose of the main element. As the turbulent boundary layer proceeds around the nose, it encounters a strong favorable pressure gradient. The accelerated boundary layer will then merge with the leading edge slat wake over the main element forming a confluent boundary layer. This thick viscous layer will then encounter an adverse pressure gradient as it moves downstream over the main element ultimately leading to flow separation, which has an unfavorable effect on $C_{L_{max}}$. However if a sufficiently strong favorable pressure gradient exists at the leading edge of the main element, the turbulent boundary layer may relaminarize, thus thinning the boundary layer and resulting in a delay of confluence. Delayed confluence will move the separation point farther aft on the main element, which has a favorable effect on $C_{L_{max}}$. Thus a possible failure of the turbulent boundary layer to relaminarize at high Reynolds number may be responsible for the inverse Reynolds number effect.

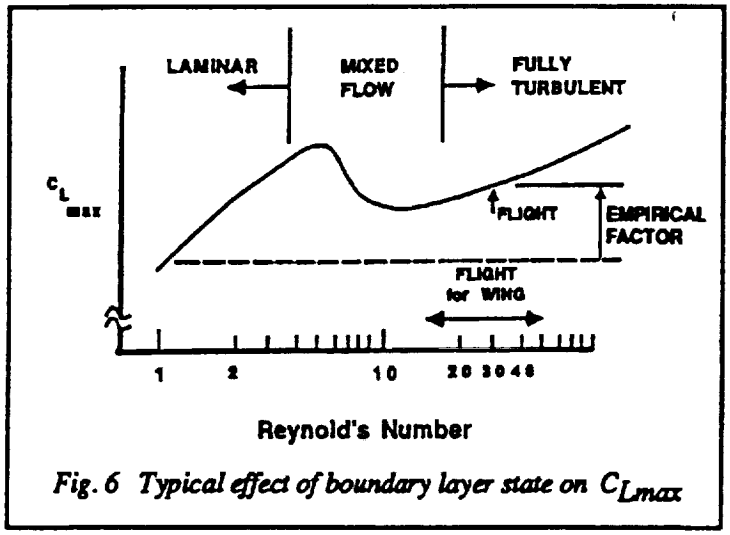

Fig. 6 Typical effect of boundary layer state on C_{Lmax}

Figure 1: Taken from Meredith, P.T., "Viscous Phenomena Affecting High-Lift Systems and Suggestions for Future CFD Development," AGARD CP-515, pp. 19-1, 19-8, 1993.

The criterion for onset of relaminarization is typically attributed to the relaminarization parameter K; a dimensionless group which results from a non-dimensionalization of the x-momentum Navier-Stokes equation and is comprised of the pressure gradient term, $\frac{dP}{dx}$, the freestream velocity, U_∞, and the kinematic viscosity, υ,. K, as defined by Launder[3], is typically written as,

$$K = \frac{\upsilon}{U_\infty^2}\frac{dU_\infty}{dx} \tag{1}$$

or K can be rewritten in terms of the pressure coefficient C_p and the Reynolds number, Re, as

$$K = -\frac{1}{2}\frac{1}{\mathrm{Re}}\left(\frac{1}{1-C_p}\right)^{\frac{3}{2}}\frac{dC_p}{dx}. \tag{2}$$

Low Reynolds numbers experiments have shown relaminarization typically occurs for values of $K \geq 3 \times 10^{-6}$. Upon inspection of the relaminarization parameter, it is evident that K is determined solely from external inviscid flow parameters and thus can be estimated using only surface pressure measurements. However one would expect that boundary layer parameters ought to influence relaminarization.

The presence of the $\frac{1}{\mathrm{Re}}$ term in Equation 2 should not be surprising if the mechanism for the inverse Reynolds number effect truly is relaminarization. In effect, at low Reynolds numbers K is large ($\geq 3 \times 10^{-6}$) and if K is the indicator for relaminarization, one would expect the leading edge turbulent boundary layer to be in a relaminarized state. Equation 2 indicates that as Reynolds number increases, K decreases and one would expect that once

the Reynolds number became large enough for the relaminarization parameter to achieve a value less than the critical value of 3×10^{-6}, relaminarization would cease. Focusing our attention on a high-lift system, at low Reynolds number, one would expect the main element turbulent boundary layer, as it moves from the attachment line around the leading edge, to relaminarize. As Reynolds number increases, a critical Reynolds number will be reached. Above this critical Reynolds number, K will drop below the critical value of 3×10^{-6}, which will lead to the cessation of relaminarization. Cessation of relaminarization will then lead to earlier confluence of the main element boundary layer and slat wake, followed by a upstream relocation of the separation point on the main element, which will result in a decrease in $C_{L_{max}}$.

1.2 University of Notre Dame/NASA Dryden Research Approach

Experiments conducted in academic wind tunnels at low Reynolds numbers have shown that for $K \geq 3 \times 10^{-6}$ relaminarization will occur. However at large Reynolds numbers, typical of those found in flight, the likelihood of relaminarization occurring is an open question. The uncertainty surrounding the importance of relaminarization in high-lift systems and the lack of fundamental knowledge of the mechanisms responsible for boundary layer relaminarization have motivated the current joint wind tunnel/flight test project between NASA Dryden Flight Research Center and the University of Notre Dame. This joint effort involves wind tunnel testing at the University of Notre Dame in support of future flight tests on the NASA Dryden FTF-II.

Two goals have been established for wind tunnel testing at the University of Notre Dame:

1. To better understand the flow physics of turbulent boundary layer relaminarization, and

2. To develop diagnostic tools in support of FTF-II flight testing at Mach and Reynolds numbers typical of commercial aircraft.

The remainder of the report will discuss how these goals were achieved and to what degree. More specifically, the following will be discussed:

1. Defining relaminarization and how best to experimentally determine when relaminarization is present,

2. Describing the relaminarization wind tunnel facility and its capabilities,

3. Documenting the experimental relaminarization results,

4. Defining a possible relaminarization design concept for the NASA Dryden FTF-II, and

5. Recommendations for future experimental measurements to further our knowledge of relaminarization and to aid in the development of the NASA Dryden FTF-II relaminarization experiment.

2 Relaminarization

2.1 Background

The first evidence of turbulent boundary layer relaminarization, or "reverse transition", was documented by Wilson and Pope 1954[4] while studying heat transfer coefficients on gas turbine blades. In the nearly five decades since Wilson and Pope's findings, there have been several important experimental investigations focusing on turbulent boundary layer relaminarization. Most notably Launder 1964[3], Patel and Head 1968[5], Blackwelder and Kovasznay 1972, Narasimha and Sreenivasan 1973[6],and more recently Fernholz and Warnack 1998[7],[8] and Ichimiya, et al. 1998 [9]. Also, an excellent review article was published by Sreenivasan[10] in 1982. The experimental investigations conducted by these researchers have provided much information regarding the processes and mechanisms associated with turbulent boundary layer relaminarization. But as will be shown, there still exists many unanswered questions surrounding the prediction of relaminarization and its occurrence outside a laboratory environment.

2.2 The Mechanics of Relaminarization

Relaminarization, or "reverse transition", occurs when a turbulent boundary layer is exposed to a large enough favorable pressure gradient over a suitable duration causing the turbulent boundary layer to revert to a laminar-like state[3],[6],[8],[10],[11],[12]. Relaminarization is characterized by: a thinning of the boundary layer, a departure of the mean velocity profiles from both the "law of the wall" and "law of the wake" profiles[5], an initial decrease then rapid increase in the shape factor[6],[11], an initial increase in the heat transfer and skin friction coefficients followed by a substantial decrease[5],[6],[11], a decrease in the relative turbulence intensity[11],[13],[14], a rapid decline of turbulent bursting in the wall-layer[15], a spread of turbulent intermittency from the outer-layer to the wall-layer[13], and a decay of the turbulent stresses in the near-wall region[8],[14].

For a boundary layer undergoing relaminarization, Launder[3] documented an energy shift toward the low wave number spectrum in the near-wall region and a similar, more pronounced, shift in the wave number spectrum of the outer-region. Indeed it has been observed that the turbulent spectra of a relaminarizing boundary layer deviates from the typical $K^{-\frac{5}{3}}$ roll-off associated with spectra of a fully developed turbulent boundary layer. The total energy associated with the relaminarized boundary layer is in fact smaller than the total energy of a fully developed turbulent boundary layer in a zero pressure gradient environment.

For a turbulent boundary layer undergoing relaminarization, Fernholz and Warnack[8] found that the integral length scales, defined as

$$\Lambda_x = \Lambda_\tau u \tag{3}$$

$$\Lambda_y = \frac{1}{2}\int_{y-\Delta y}^{y+\Delta y} R_{u'u'} d\Delta y \tag{4}$$

where Λ_τ is defined as

$$\Lambda_\tau = \int_0^\tau R_\tau d\tau \tag{5}$$

show an increase in Λ_x/δ by a factor of four and an increase in Λ_y/δ by a factor of two over a typical turbulent boundary layer in zero pressure gradient. An elongation of the large eddy structure in the streamwise direction due to the large favorable pressure gradient is also evident in a relaminarized turbulent boundary layer. These elongated large scale structures show no evidence of scaling with the boundary layer thickness, δ, as they do in zero and adverse pressure gradients. When emerging from the strong favorable pressure gradient region into a zero pressure gradient environment, the large scale structure contain definite history effects attributed to flow acceleration.

2.3 A Model For Relaminarization

In describing the sequence of events that would lead to relaminarization, Launder[3] commented that as a turbulent boundary layer is exposed to a large favorable pressure gradient the turbulent structure in the near-wall region begins to depart from its fully turbulent state. The turbulent boundary layer becomes unable to respond to the large flow acceleration and a rapid momentum increase results. This increase in momentum causes an increase in the viscous shear stress, which if the pressure gradient persists, grows larger than the turbulent stress due to the inability of the turbulent structure to adjust to the flow acceleration. Consequently, the turbulence dissipation exceeds production, which leads to a decay of the turbulent structure, resulting in relaminarization.

Elaborating on Launder's premise, Sreenivasan[10] incorporated a two-layer model comprised of a viscous inner-layer and an inviscid outer-layer to explain the mechanism responsible for relaminarization. Sreenivasan argued that when a turbulent boundary layer is exposed to a large favorable pressure gradient, the turbulent structure is distorted in the outer-layer by the rapid flow acceleration. During this rapid acceleration, a new viscous inner-layer develops in which the initial turbulence decays. Unlike the inner-layer, turbulence decay in the outer-layer is insignificant. The two layers interact weakly, in so far as they only provide the appropriate boundary conditions. The major contributor to relaminarization in this view is the "domination of pressure forces over the slowly responding Reynolds stresses in the outer-layer, accompanied by the generation of a new laminar subboundary layer, which itself is maintained stable by the acceleration."

2.4 A Criterion for Relaminarization

Relaminarization is not a catastrophic phenomenon and, as such, the onset of relaminarization is invariably difficult to define. In his 1982 review paper, Sreenivasan[10] assembled a number of the typical parameters that have been used to define the onset of relaminarization;

Parameter	Numerical Value
K	$\simeq 3.0\ x\ 10^{-6}$
Δp	$\simeq -0.025$
$\Delta\tau$	$\simeq 0.025,\ n = -\frac{3}{2}$
Kc_f^n	$\simeq 0.025,\ n = -\frac{3}{2}$
H	$\min(H)$

Table 1: Common relaminarization parameters and their values at the onset of relaminarization

they include K, Δp, $\Delta\tau$, Kc_f^n, and H where these quantities are defined as

$$K = \frac{\nu}{u^2}\frac{du}{dx} \tag{6}$$

$$\Delta p = \frac{\nu}{u_\tau^3}\frac{dP}{dx} \tag{7}$$

$$\Delta\tau = \frac{\nu\frac{\partial\left(\overline{-uv}\right)}{\partial y}}{u_\tau^3} \tag{8}$$

$$Kc_f^n = \frac{\nu}{u^2}\frac{du}{dx}c_f^n \tag{9}$$

$$H = \frac{\delta^*}{\theta} \tag{10}$$

Typical values of the above parameters used as indicators of relaminarization are listed in Table 1.

Narayanan and Ramjee[11] observed the onset of relaminarization to correspond with a decrease in the turbulence intensity. They also observed the disappearance of turbulent bursts near the wall occurring for similar values of the above relaminarization parameters. In addition to the previously mentioned criteria, Fernholz and Warnack[8] recently documented two higher moments, the skewness, $S_{\tau_{w'}}$, and the flatness, $F_{\tau_{w'}}$, of the fluctuating skin friction coefficient reaching maximums at the initiation of relaminarization.

Although the above parameters are useful in approximately determining the onset of relaminarization, they are often not adequate enough and offer little to no help in explaining why a turbulent boundary layer will relaminarize. In fact, Sreenivasan[10] comments "...these criteria are often useful as rough indicators of some drastic changes in the accelerated turbulent boundary layer." And "...that the convenience associated with the use of any of these criteria should not mask our concern about their basic inadequacy as markers of the 'onset' of relaminarization." Also Narasimha[6] writes "...it would be somewhat surprising if, over an appreciable Reynolds number range, the relevant parameter were to be one like K which takes no account of the shear flow at all."

3 Experimental Work Completed

3.1 Relaminarization Test Facility

To explore the role of relaminarization in high-lift systems and to gain a better under-

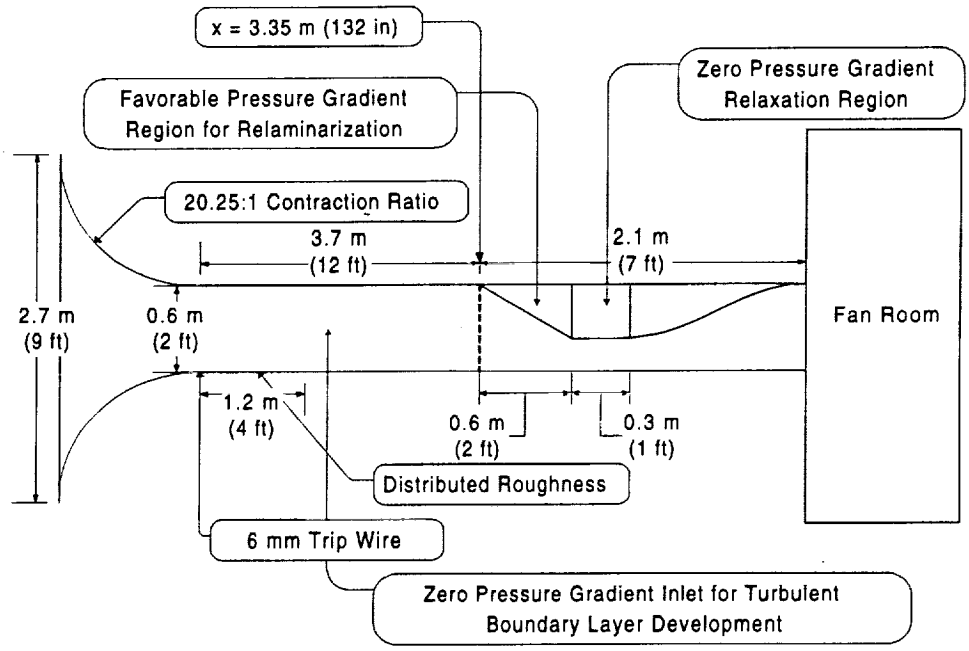

Figure 2: Hessert Center relaminarization wind tunnel test facility.

standing of the mechanism(s) responsible for relaminarization, a wind tunnel test facility was constructed at the Hessert Center utilizing the $0.6\,\mathrm{m} \times 0.6\,\mathrm{m}$ $(2\,\mathrm{ft} \times 2\,\mathrm{ft})$subsonic indraft wind tunnels. The design of the wind tunnel test section was motivated by the desire to expose a turbulent boundary layer to a region of favorable pressure gradient corresponding to a constant K value. Inspection of Equation 2 reveals that at a fixed Reynolds number, to maintain a constant value of K over a specified streamwise distance, it is necessary that.

$$\left(\frac{1}{1-C_p}\right)^{\frac{3}{2}} \frac{dC_p}{dx} = C \tag{11}$$

where C is a constant. Invoking conservation of mass and the definition of C_p it can be shown that the required tunnel geometry to maintain a constant value of K is a linear profile given by,

$$h(x^*) = h_o\,(1 - K\,\mathrm{Re}_L\,x^*) \tag{12}$$

where h is the height of the wind tunnel section, h_o is the initial height of the converging section, Re_L is the Reynolds number based on L, the length of the converging section, and

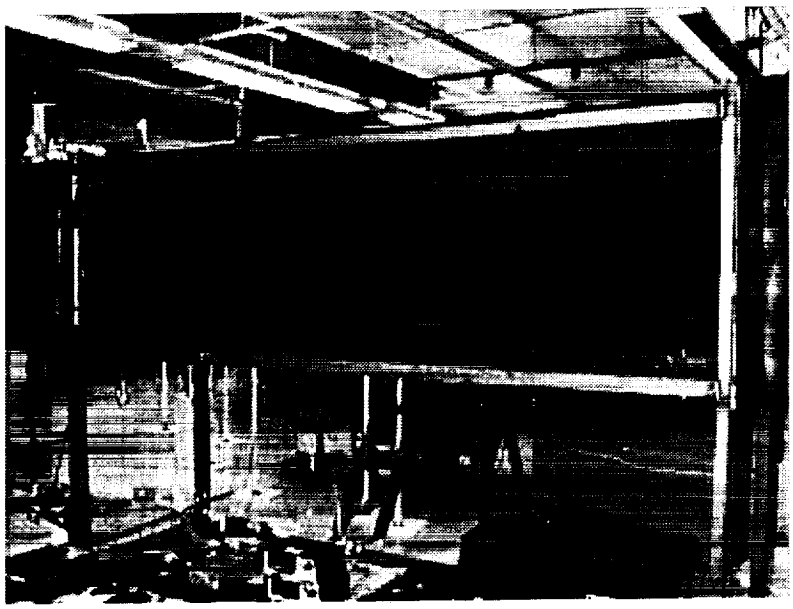

Figure 3: Side view of the current relaminarization wind tunnel facility at the University of Notre Dame.

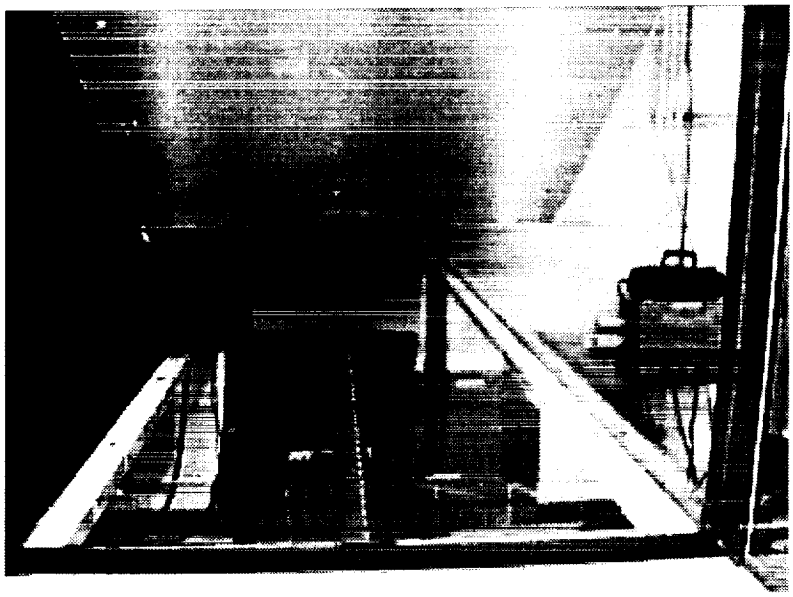

Figure 4: Internal view of the converging section of the relaminarization wind tunnel facility at the University of Notre Dame.

x^* is the streamwise distance non-dimensionalized by L. Equation 12 implies that for a fixed tunnel geometry, changing the freestream velocity results in changing the value of K. Thus the wind tunnel section was designed to provide a constant K value over a distance of 2 ft for a range of velocities that would correspond to values of K between approximately 5×10^{-6} and 1×10^{-6}; values large enough to obtain relaminarization and values small enough where one would expect relaminarization not to occur. Figure 2 provides a schematic of the current relaminarization test facility, while Figure 3 is a side photograph of the wind tunnel test section and Figure 4 is a photograph showing an internal view of the converging section.

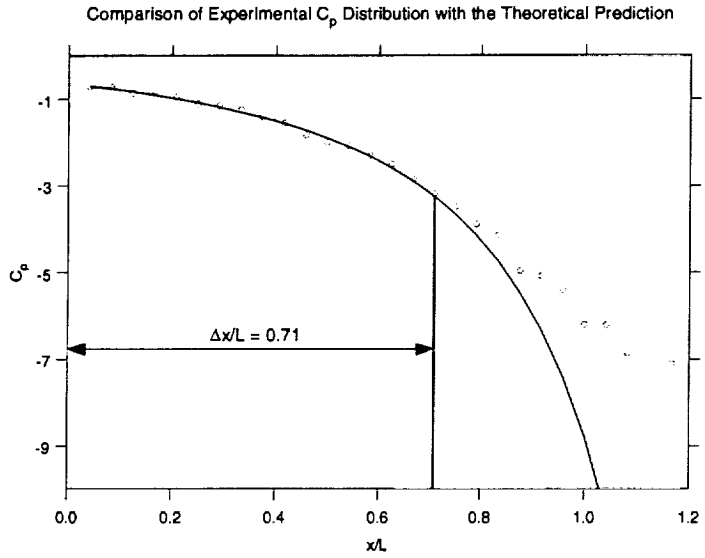

Figure 5: Theoretical prediction of C_p distribution overlayed on experimental C_p curve. Demonstrates a region of approximately 0.43 m (17 in) where K is constant.

Figure 5 contains a plot of the theoretical pressure distribution for a constant value of K compared with the experimental pressure distribution measured in the converging section of the wind tunnel. The theoretical pressure distribution is represented by the solid curve in Figure 5 and is described by

$$C_p\left(\frac{x}{L}\right) = (1 + C_{p_{x=3.35\,\mathrm{m}}}) - \left(\frac{1}{1 - K\,\mathrm{Re}_L\left(\frac{x}{L}\right)}\right)^2 \tag{13}$$

which satisfies the relation in Equation 11. The data points in Figure 5 represent the experimentally measured coefficient of pressure in the converging section of the wind tunnel. The theoretical and experimental pressure distributions are in acceptable agreement over a range of approximately 0.43 m (17 in), which corresponds to

$$\frac{\Delta x}{L} = \frac{0.43\,\mathrm{m}}{0.61\,\mathrm{m}} = 0.71 \tag{14}$$

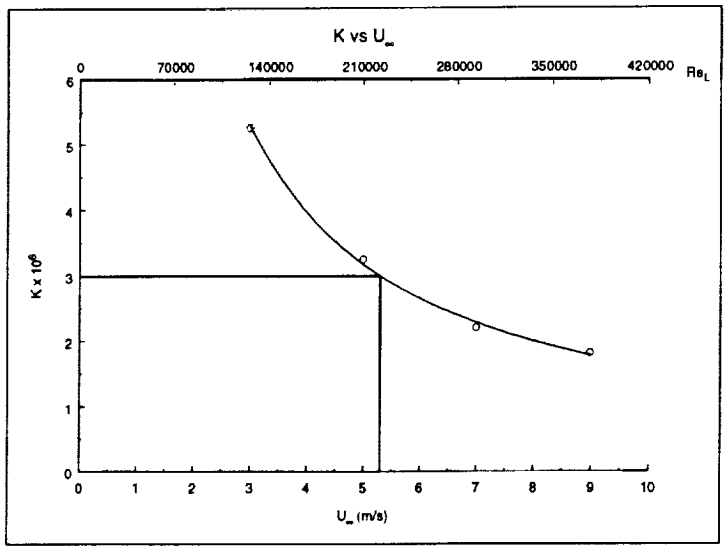

Figure 6: Range of attainable K values for corresponding wind tunnel freestream velocities. $K = 3 \times 10^{-6}$ corresponds to $\mathrm{Re}_L \sim 220,000$.

or 71% of the converging section of the wind tunnel (where L is the length of the converging section). This demonstrates that the facility has the ability to maintain a region of constant K over approximately this streamwise distance (0.43 m (17 in)). This length is found to be remarkably consistent over the designed operating range of the wind tunnel test section. Figure 6 illustrates the attainable K values for the designed operating range of the wind tunnel facility.

3.2 Experimental Results from the Relaminarization Test Facility

3.2.1 Initial Conditions

To document relaminarization and determine the mechanisms responsible for relaminarization, it is necessary to have a fully developed turbulent boundary layer. Thus the first tests conducted in the relaminarization facility involved documenting the development and state of the initial boundary layer upstream of the favorable pressure gradient region. Maintaining a turbulent boundary layer throughout the operating velocity range was more difficult than first thought. Many changes to the boundary layer development region were explored to ensure a fully developed turbulent boundary layer was present upstream of the relaminarization region.

Using a 90° X-wire boundary layer probe, a full flow field survey was conducted upstream of the relaminarization region to document the boundary layer state. Because the flat plate boundary layer develops in a nominally zero pressure gradient environment upstream of the

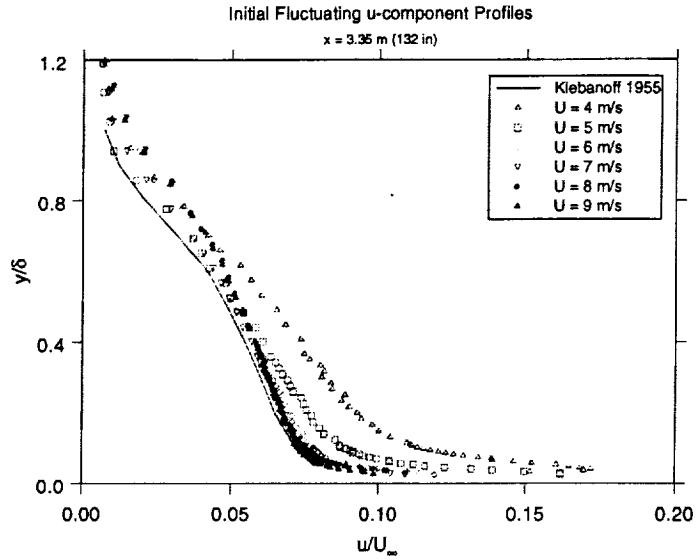

Figure 7: u/U_∞ velocity profiles at $x = 3.35\,\mathrm{m}$ $(132\,\mathrm{in})$ for $U_\infty = 4, 5, 6, 7, 8, 9\ \frac{\mathrm{m}}{\mathrm{s}}$.

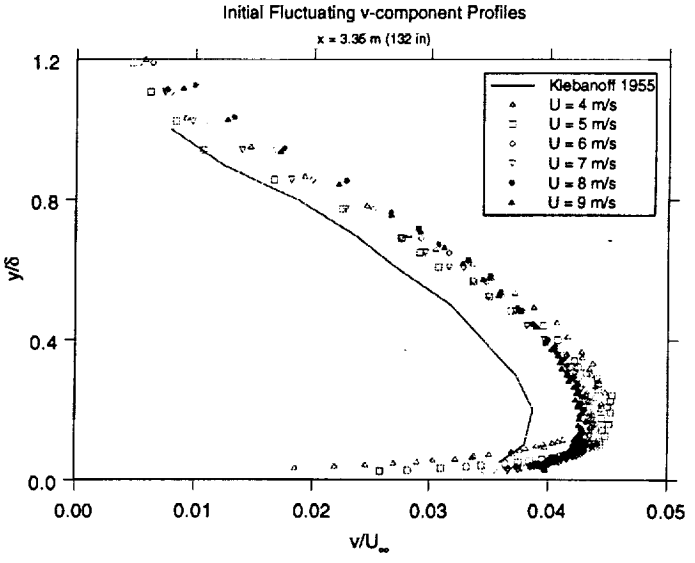

Figure 8: v/U_∞ velocity profiles at $x = 3.35\,\mathrm{m}$ $(132\,\mathrm{in})$ for $U_\infty = 4, 5, 6, 7, 8, 9\ \frac{\mathrm{m}}{\mathrm{s}}$.

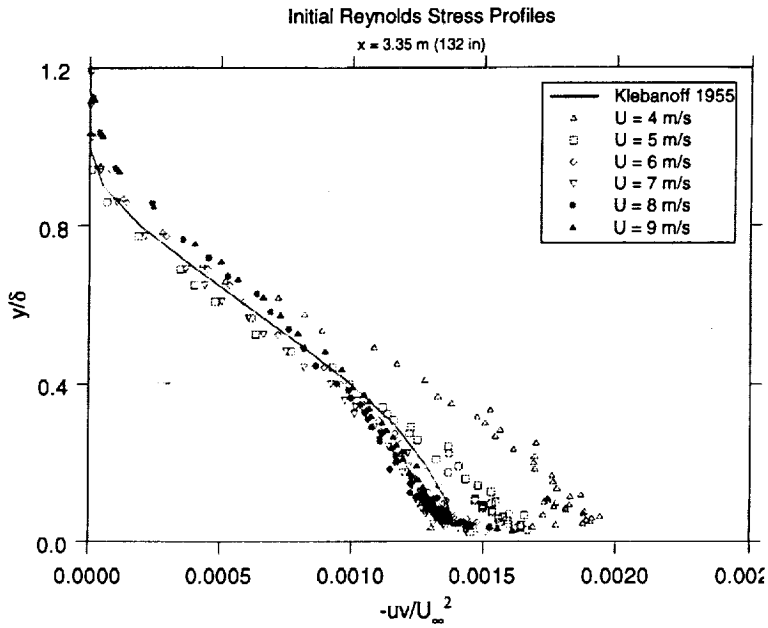

Figure 9: $-\overline{uv}/U_\infty$ velocity profiles at $x = 3.35\,\mathrm{m}$ (132 in) for $U_\infty = 4, 5, 6, 7, 8, 9\ \frac{\mathrm{m}}{\mathrm{s}}$.

relaminarization region, the fluctuating velocity profiles were compared to Klebanoff's[16] 1955 data for a fully developed turbulent boundary layer on a flat plate. Figure 7 is a plot of the turbulence intensity versus the normal distance from the wall nondimensionalized by the local boundary layer thickness. Figure 8 is plot of the fluctuating v velocity scaled by the freestream velocity plotted versus the normal distance from the wall nondimensionalized by the local boundary layer thickness. Figure 9 is plot of the Reynolds stress plotted versus the normal distance from the wall nondimensionalized by the local boundary layer thickness. In Figures 7-9, the profiles shown are for $4 \leq U_\infty \leq 9 \frac{\mathrm{m}}{\mathrm{s}}$ at $x = 3.35\,\mathrm{m}$ (132 in) (the location directly upstream of the converging section of the wind tunnel) and Klebanoff's profiles are also plotted for comparison.

The turbulence intensity profiles (Figure 7) shows good agreement with Klebanoff's data for $6 \leq U_\infty \leq 9 \frac{\mathrm{m}}{\mathrm{s}}$. The $U_\infty = 4,5 \frac{\mathrm{m}}{\mathrm{s}}$ deviate from the other profiles for $0 \leq y/\delta \leq 0.5$. Likewise, the Reynolds stress profiles in Figure 9 display good agreement with Klebanoff's data. The fluctuating normal velocity component profiles show good agreement with one another, but are shifted off Klebanoff's curve; this is believed to be a bias error caused by alignment of the X-wire probe.

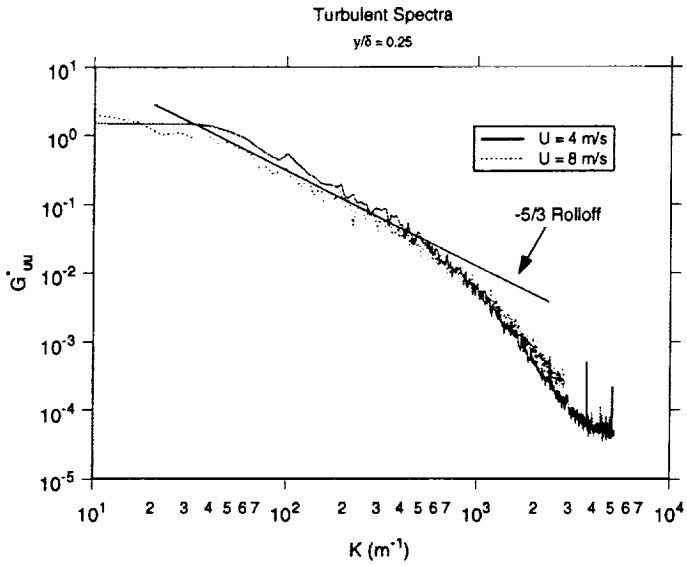

Figure 10: Turbulent u component velocity spectra comparison for $U_\infty = 4 \frac{\mathrm{m}}{\mathrm{s}}$ and $U_\infty = 8 \frac{\mathrm{m}}{\mathrm{s}}$ at $x = 3.35\,\mathrm{m}$ (132 in).

The discrepancy between the measured profiles, specifically $U_\infty = 4 \frac{\mathrm{m}}{\mathrm{s}}$, led to an examination of the turbulent spectra. The u-component velocity spectra for $U_\infty = 4 \frac{\mathrm{m}}{\mathrm{s}}$ and $U_\infty = 8 \frac{\mathrm{m}}{\mathrm{s}}$ is plotted in Figure 10 and clearly the turbulent spectra exhibit a region in which the roll-off is consistent with the expected $K^{-\frac{5}{3}}$ for turbulent boundary layers. Thus based on the behavior of the mean profiles and an examination of the turbulent spectra, it was concluded that for all initial velocities in the range of $4 \frac{\mathrm{m}}{\mathrm{s}} \leq U_\infty \leq 9 \frac{\mathrm{m}}{\mathrm{s}}$ there was indeed a

U_∞ $\left[\frac{m}{s}\right]$	δ $[mm]$	θ $[mm]$	δ^* $[mm]$	H	Re_θ	C_f	U_τ $\left[\frac{m}{s}\right]$
4	60.0	6.08	8.91	1.47	1545	0.00390	0.1639
5	57.5	5.33	7.41	1.39	1770	0.00400	0.2168
6	60.0	5.86	7.85	1.34	2344	0.00380	0.2548
7	60.0	5.41	7.22	1.34	2556	0.00375	0.2990
8	60.0	5.31	7.08	1.33	2839	0.00370	0.3359
9	60.0	5.12	6.85	1.34	3042	0.00365	0.3711

Table 2: Summary of boundary layer parameters for the initial turbulent boundary layer at $x = 3.35\ m$ $(132\ in)$

initially turbulent boundary layer present. Table 2 contains a summary of several boundary layer parameters for the initial turbulent boundary layer at $x = 3.35\,\mathrm{m}$ $(132\,\mathrm{in})$.

3.2.2 Relaminarization Results

While testing was conducted for six discrete K values, results will be discussed for only two cases:

1. $K = 4.10 \times 10^{-6}, \quad U_\infty = 4 \frac{\mathrm{m}}{\mathrm{s}}$
2. $K = 2.05 \times 10^{-6}, \quad U_\infty = 8 \frac{\mathrm{m}}{\mathrm{s}}$

For Case 1, we would expect to observe relaminarization since $K \geq 3.0 \times 10^{-6}$, however for Case 2 we would not expect to see relaminarization since $K \leq 3.0 \times 10^{-6}$. Examining Figure 11, a plot of the boundary layer thickness evolution, it is apparent that the Case 1 boundary layer thins at a greater rate than the Case 2 boundary layer. The Case 1 boundary layer also is thinner than the Case 2 boundary layer in the converging section although the Case 2 boundary layer is moving at twice the initial velocity; this is consistent with relaminarization occurring in the Case 1 boundary layer. Focusing on the shape factor evolution, where

$$H = \frac{\delta^*}{\theta} \tag{15}$$

inspection of Figure 12 reveals similar trends between the Case 1 and Case 2 boundary layers. At the onset of relaminarization, we would expect to see a sharp decline in the shape factor, in fact reaching a minimum value, followed by a gradual increase. Case 1 demonstrates this behavior in the region of $x = 3.94\,\mathrm{m}$ $(155\,\mathrm{in})$, but it is not apparent to the author how to differentiate between the behavior in Case 1 and Case 2 as relaminarization and no relaminarization present. Examination of the skin friction values in Figure 13 shows a large decrease in the Case 1 boundary layer in the region of $x = 3.94\,\mathrm{m}$ $(155\,\mathrm{in})$ when compared to the Case 2 boundary layer. This behavior is consistent with the onset of relaminarization in the Case 2 boundary layer. Figure 14 illustrates the evolution of the maximum turbulence intensity; it is evident that the Case 1 boundary layer sees a reduction and maintenance in turbulence intensity levels when compared to the Case 2 boundary layer, which continues to grow with downstream distance. This behavior would suggest relaminarization occurring in the Case 1 boundary layer. Finally, examining the log-law profiles in Figure 15, there is a noticeable deviation from the expected log-law behavior in the $x = 3.94\,\mathrm{m}$ $(155\,\mathrm{in})$ plot; typical of a boundary layer undergoing relaminarization as observed by Patel and Head[5]. However, this behavior is observed for both Case 1 and 2 when one would expect only to see a deviation in the Case 1 boundary layer, if deviation of the boundary layer profile from the typical log-law profile is a proper criterion for the onset of relaminarization. In fact, Fernholz and Warnack[7] found similar deviations in log-law behavior for boundary layers in favorable pressure gradients with $K \leq 3.0 \times 10^{-6}$ and no observable relaminarization.

From the above data, it is obvious to see that determining the onset of relaminarization is a great challenge. An objective analysis of the data yields no conclusive results indicating where and when relaminarization occurs. In fact after analyzing similar data sets for values of K between $1 \times 10^{-6} \leq K \leq 5.0 \times 10^{-6}$, it becomes apparent that relaminarization does not have a readily identifiable dependence on K. Most quantities change continuously with increasing K; demonstrating no catastrophic changes when relaminarization is present. Therefore the need arises for a more suitable method of detecting relaminarization.

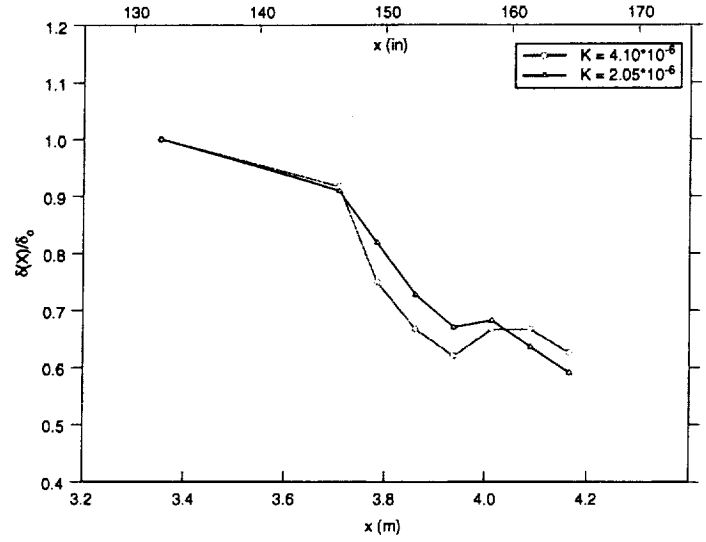

Figure 11: Boundary layer thickness evolution for $K = 4.10 \times 10^{-6}$ and $K = 2.05 \times 10^{-6}$.

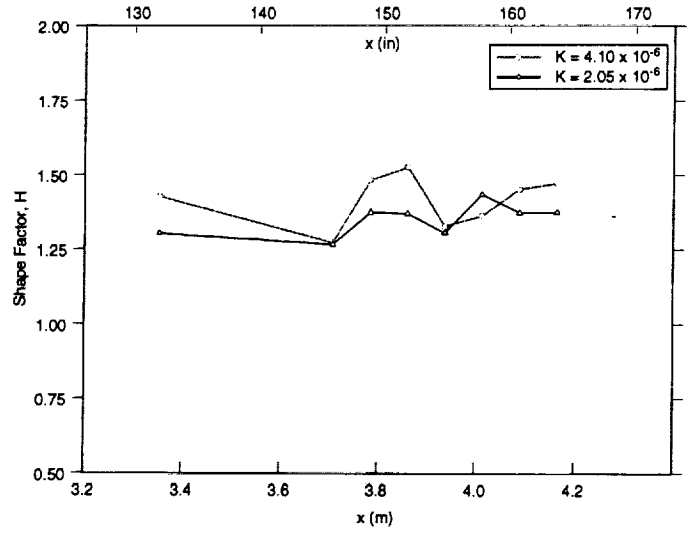

Figure 12: Boundary layer shape factor evolution for $K = 4.10 \times 10^{-6}$ and $K = 2.05 \times 10^{-6}$.

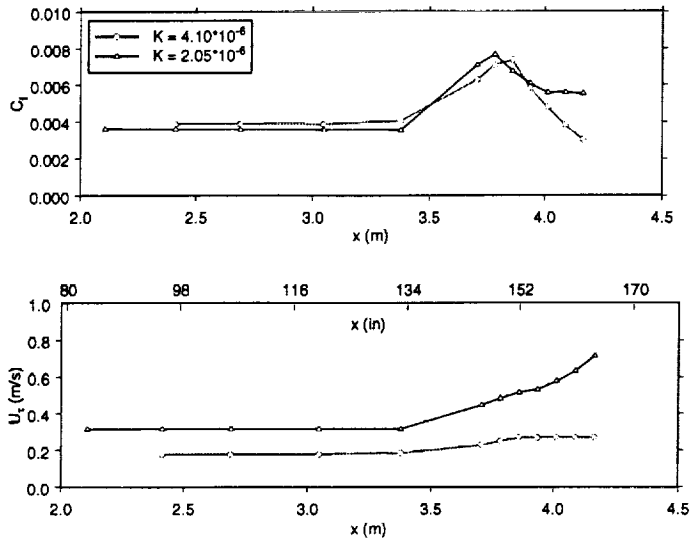

Figure 13: Boundary layer skin friction and friction velocity evolution for $K = 4.10 \times 10^{-6}$ and $K = 2.05 \times 10^{-6}$.

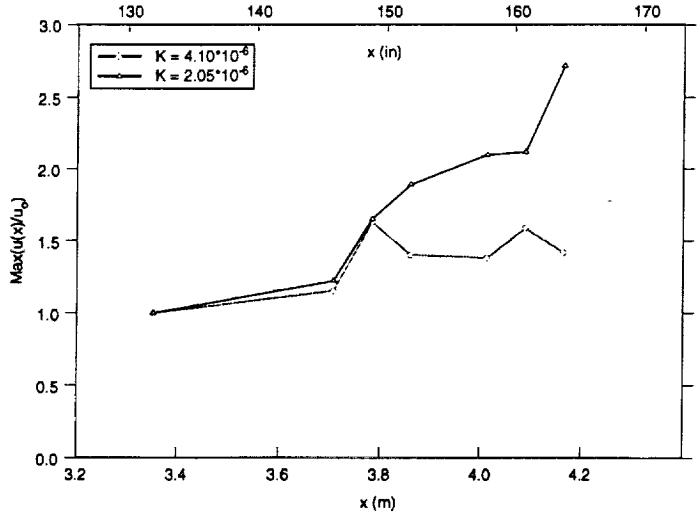

Figure 14: Maximum turbulence intensity evolution for $K = 4.10 \times 10^{-6}$ and $K = 2.05 \times 10^{-6}$.

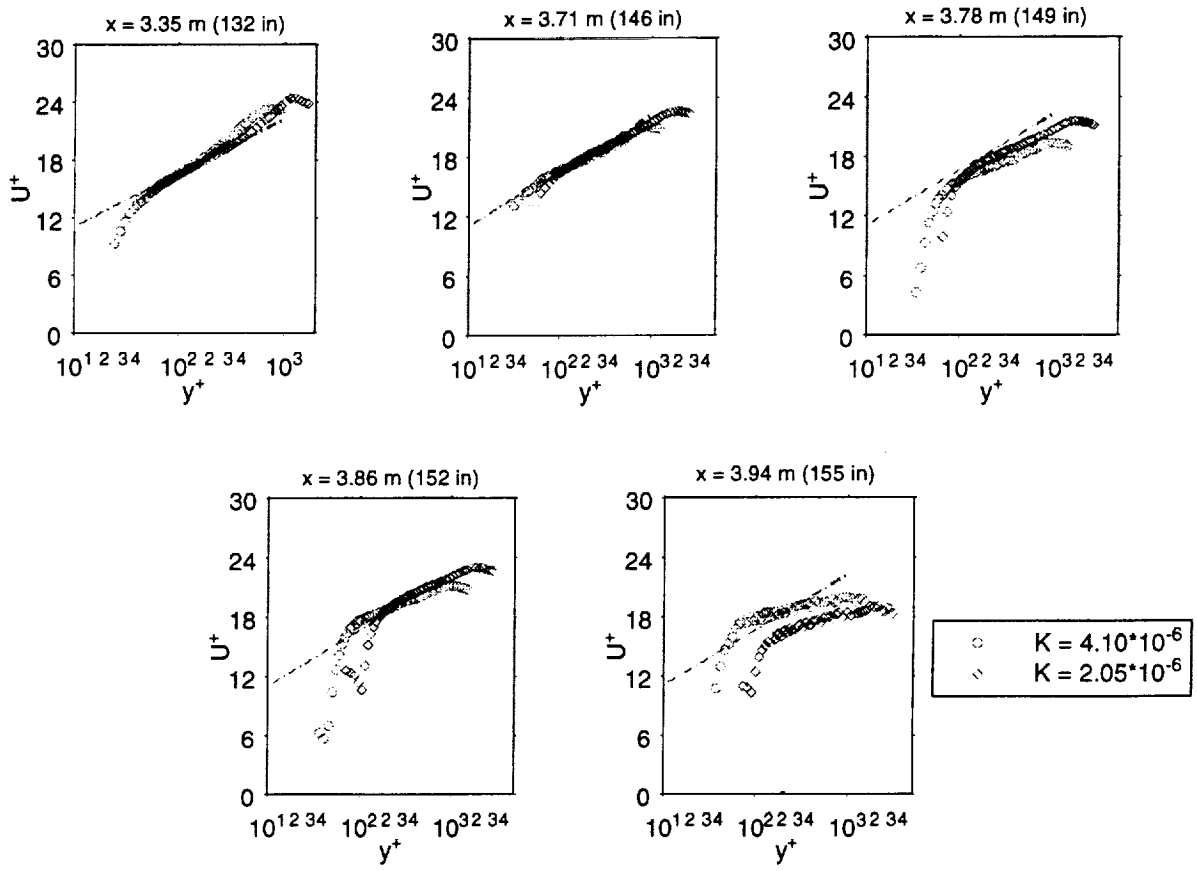

Figure 15: Log-law profiles at various streamwise locations for $K = 4.10 \times 10^{-6}$ and $K = 2.05 \times 10^{-6}$.

3.2.3 Turbulent Burst-Sweep Event Detection

As previously stated, relaminarization of a turbulent boundary layer is thought to be caused by the domination of the pressure forces over the slowly responding Reynolds stresses[3],[6],[10], but as Fernholz and Warnack[8] found, "this result excludes a parameter-connected criterion for the onset of relaminarization and for the breakdown of the standard logarithmic law." These results are consistent with the current findings of this study. Indeed, this poses a serious problem if we are to assess the influence of relaminarization on any given engineering problem.

In search for a better understanding of the flow physics associated with turbulent boundary layers exposed to large favorable pressure gradients, Fernholz and Warnack [7],[8] made detailed flow field measurements and documented the turbulent properties of the boundary layer. They found a gradual change in the turbulence properties of the turbulent boundary layer when exposed to large favorable pressure gradients; consistent with the claim that the relaminarization process is not a catastrophic event. In addition, Fernholz and Warnack[8] documented a significant change in the near-wall turbulence quantities for a relaminarizing turbulent boundary layer. Focusing on the fluctuating wall shear stress, they found large changes in the lower and higher moments, skewness, flatness, and the Reynolds normal stress in the near-wall region ($y^+ < 20$). These significant changes in the near-wall region may be indicative of large changes in the turbulent burst-sweep cycle of events. If so, the turbulent bursting rate is a measurable quantity and may well be a significant factor in determining the onset of relaminarization.

Using Quadrant Splitting Analysis, a conditional sampling technique often used to detect burst-sweep events, the turbulent bursting frequency can be computed from time signals of fluctuating u and v velocity measured via an X-wire in the near-wall region. The turbulent bursting frequency is defined as the time between ejections and can be nondimensionalized as

$$T_B^+ = \frac{T_B U_\infty}{\delta} \tag{16}$$

using the freestream velocity and the boundary layer thickness. The higher the turbulent burst frequency, the larger the time between detected burst-sweep events, or, in other words, the lower the turbulent burst rate.

Applying Quadrant Splitting Analysis to the u and v time signals measured in the near-wall region of the wind tunnel, the turbulent burst frequency is extracted and is plotted in Figure 16. For the Case 2 ($K = 2.05 \times 10^{-6}$) boundary layer, there is a slight increase in the turbulent burst frequency through the contraction; this indicates a slight decrease in the turbulent burst rate as the flow travels through the contraction and is most likely explained by the presence of the strong favorable pressure gradient acting as a stabilizing influence on the turbulence production. For the Case 1 ($K = 4.10 \times 10^{-6}$) boundary layer, the turbulent burst frequency follows the Case 2 flow until approximately $x = 3.94\,\text{m}$ (155 in) where the burst frequency dramatically increases before relaxing to the exit values of Case 2. This increase in the burst frequency is associated with a large reduction in the turbulent bursting rate; a large reduction in turbulent bursting rate is consistent with relaminarization of the turbulent boundary layer. Tentatively, it seems the strong favorable pressure gradient acts

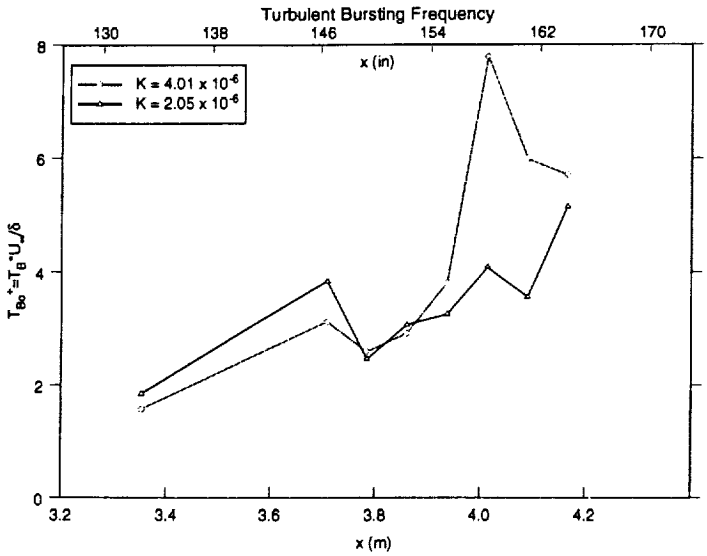

Figure 16: Turbulent burst frequency evolution calculated using Quadrant Splitting Analysis.

to reduce the bursting rate in a turbulent boundary layer slightly, but imposed on this mild reduction in a turbulent boundary layer is an even larger reduction in the turbulent bursting rate when relaminarization is present.

4 Relaminarization and the NASA Dryden FTF-II

4.1 Design Concept

The flight testing phase of the project is designed to determine the flow physics of turbulent boundary layers undergoing relaminarization at Reynolds and Mach numbers typical of high-lift systems found on commercial aircraft. In keeping with this focus, the flight test model on the FTF-II must approximate the pressure gradient and flow field found on the main element leading edge in these high-lift systems. The current design incorporates the upper half of the FTF-II with a horizontal splitter plate mated to the FTF-II. The horizontal splitter plate has a rounded leading edge which acts to accelerate the flow around the leading edge. To supplement this flow acceleration, a symmetric airfoil is mounted below the leading edge nose. The leading edge boundary layer is exposed to the favorable pressure gradient, which is associated with the off-surface airfoil suction peak. It is proposed that the airfoil be mounted to a servo motor thereby allowing the airfoil to be pitched while in-flight and increasing the number of tests that can be performed per flight. This design concept is illustrated in Figure 17.

A preliminary analysis using a commercially available panel code has been performed on a representative model with a cylindrical leading edge for a small number of configurations.

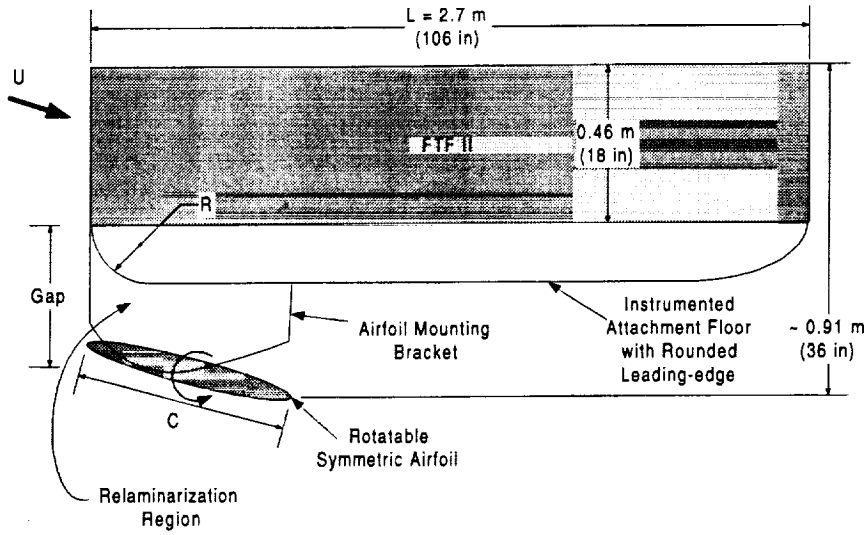

Figure 17: FTF-II flight test schematic featuring horizontal splitter plate with rounded leading edge and rotatable symmetric airfoil for modifying pressure field.

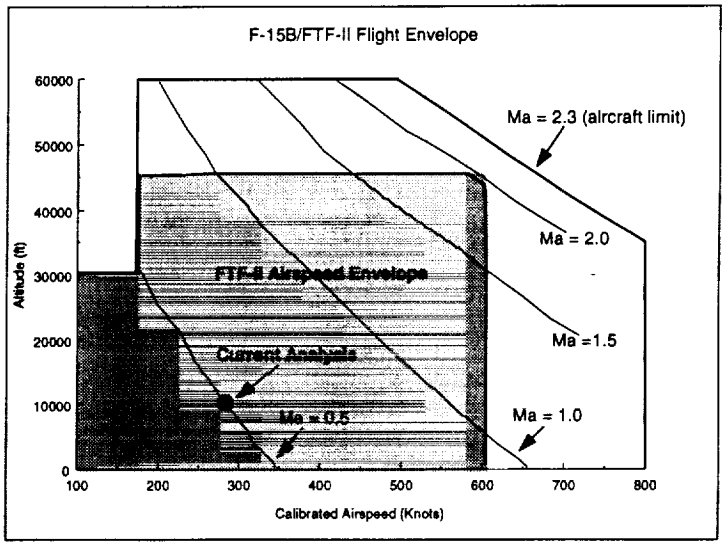

Figure 18: F-15B/FTF-II flight envelope with the current computational analysis location indicated.

All calculations were performed assuming a Mach number, $M_\infty = 0.5$, at an altitude of 10,000 ft as indicated in Figure 18. This corresponds to a unit Reynolds number for the FTF-II of $\mathrm{Re} = 7.57 \times 10^6$. Two leading edge radii were chosen, $R/L = 0.1$ and $R/L = 0.2$, (where $L = 2.69\,\mathrm{m}$ (106 in) is the length of the FTF-II). The chord of the symmetric airfoil was chosen to be $c/L = 0.3$ and the thickness to be $t/L = 0.05$ for both cases. The gap, defined as the distance between the leading edge of the main body (FTF-II) and the leading edge of the symmetric airfoil at zero angle of attack relative to the main body, was chosen to be $gap/L = 0.2$ and $gap/L = 0.3$ for the 10% and 20% radius case respectively. For both leading edge radii, computations were made at angles of attack of 0°, 5°, and 10° with respect to the main body. Figure 19 shows a plot of the relaminarization parameter K vs. non-dimensional distance, x/L, for the $R/L = 0.1$ leading edge radius at the three angles of attack denoted previously. The value of $K = 3 \times 10^{-6}$ is indicated as well. Clearly Figure 19 indicates sufficiently large values of the relaminarization parameter to achieve relaminarization on the leading edge, if K is the appropriate governing parameter. Figure 20 is a similar plot for the $R/L = 0.2$ leading edge radius and it also indicates the ability to achieve relaminarization on the leading edge, if, again, K is indeed the appropriate parameter. Therefore, with a simple model configuration such as the one illustrated in Figure 17, sufficiently strong flow acceleration can be developed to achieve relaminarization on the FTF-II assuming K is the appropriate design variable.

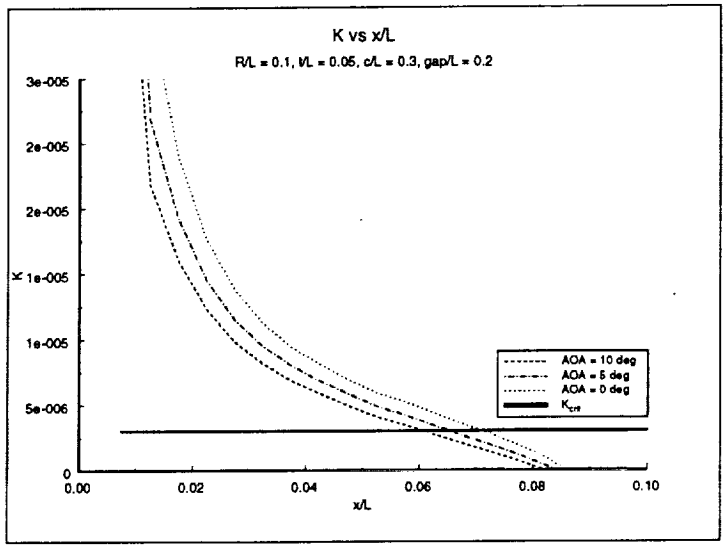

Figure 19: Computation #1 on FTF-II model leading edge indicating K values large enough to achieve relaminarization.

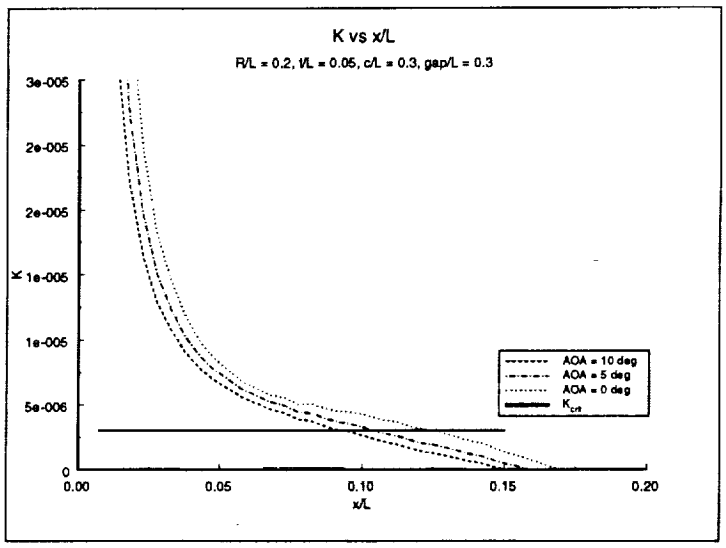

Figure 20: Computation #2 on the FTF-II model leading edge indicating a K value large enough to achieve relaminarization.

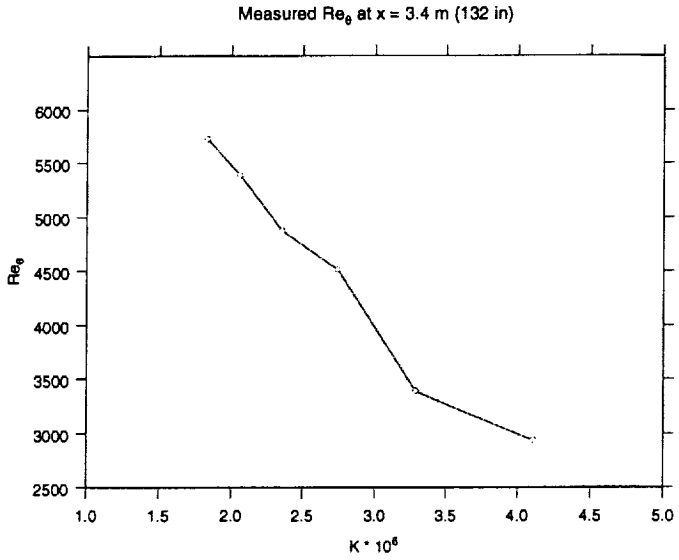

Figure 21: Re_θ behavior for given acceleration parameter K.

5 Recommendations

5.1 Short Coming's of the Relaminarization Test Facility

While the relaminarization test facility has yielded valuable data, there are several concerns regarding the current approach. Chief among these is the unavoidable fact that to achieve increasing values of the acceleration parameter K, the initial Reynolds number must decrease, as can be seen in Figure 21. The problem exists because the larger K values are achieved at relatively small velocities, which makes sustaining a fully developed turbulent boundary layer difficult. In fact, there is evidence which suggests the presence of low Reynolds number effects in the initial turbulent boundary layer for the $U_\infty = 4\ \frac{\mathrm{m}}{\mathrm{s}}$ and $U_\infty = 5\ \frac{\mathrm{m}}{\mathrm{s}}$ cases. These effects can be seen in Figures 7-9 and 15. In addition, by decreasing the initial Reynolds number to achieve greater values in the acceleration parameter, the effect of pressure gradient becomes more and more dominant over a turbulent boundary layer whose turbulence is becoming weaker; making it difficult to make definitive statements about the effect of K on relaminarization.

5.2 A New Relaminarization Facility

Future work will focus on the design and construction of a new relaminarization facility in the University of Notre Dame's Hessert Center's $1.5\,\mathrm{m} \times 1.5\,\mathrm{m}$ ($5\,\mathrm{ft} \times 5\,\mathrm{ft}$) atmospheric wind tunnel. The reasons for moving from the current $0.6\,\mathrm{m} \times 0.6\,\mathrm{m}$ ($2\,\mathrm{ft} \times 2\,\mathrm{ft}$) indraft wind tunnel are threefold:

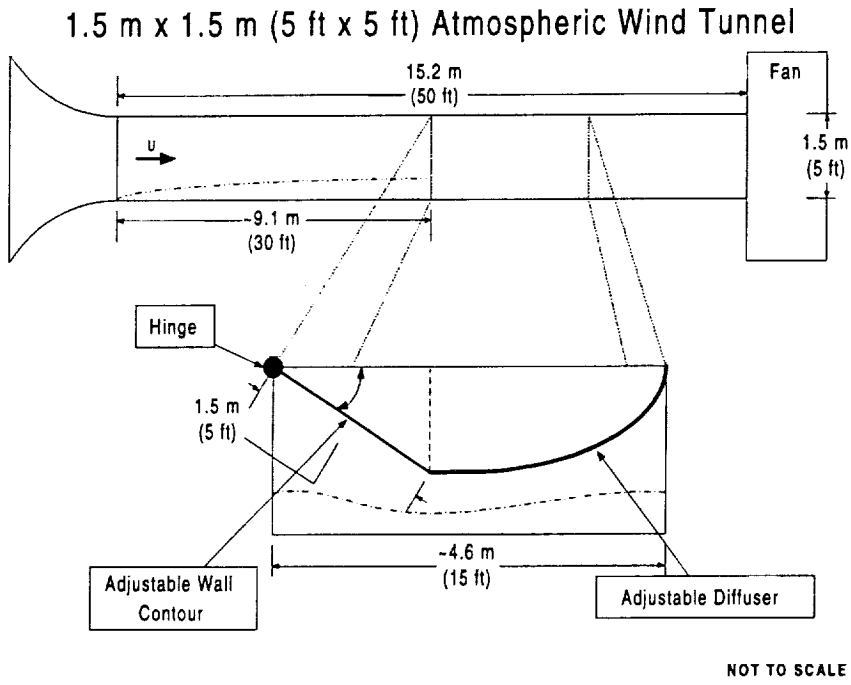

Figure 22: Schematic drawing of proposed relaminarization test facility in 1.5 m $\times$1.5 m (5 ft $\times$5 ft) atmospheric wind tunnel.

1. Operate with a fixed initial and higher Re_θ while maintaining a variable K environment through the use of a adjustable wall contour,

2. Increase the initial Reynolds number to ensure a fully turbulent boundary layer,

3. Increase the initial boundary layer thickness to allow for greater wall-normal spatial resolution in the measurements.

In the current facility, to achieve greater values of the acceleration parameter, K, the initial Reynolds number must decrease. To address this problem, the new test facility will incorporate a adjustable wall contour. Maintaining the linear contour used in the current 0.6 m $\times$0.6 m test facility to achieve a constant K environment, the 1.5 m $\times$1.5 m test facility's linear contour will be hinged at the ceiling and the angle of inclination to the top wind tunnel wall will be adjustable. Figure 22 is a schematic of the proposed relaminarization test facility in the 1.5 m $\times$1.5 m atmospheric tunnel. Unlike the current test facility in which selection of the initial Reynolds number dictates the K value, adjustment of the wall contour in the 1.5 m $\times$1.5 m test facility will provide the desired K value for any prescribed initial Reynolds number.

It is planned to conduct the relaminarization experiments in the 1.5 m $\times$1.5 m atmospheric tunnel with an initial velocity of $U_\infty = 5\ \frac{\mathrm{m}}{\mathrm{s}}$, which corresponds to a initial Reynolds number of $Re_\theta = 5660$. Three constant values of the acceleration parameter will be studied:

1. mild favorable, $K \simeq 1.5 \times 10^{-6}$
2. moderate favorable, $K \simeq 3.5 \times 10^{-6}$
3. strong favorable, $K \simeq 5.0 \times 10^{-6}$.

In 1998, Fernholz and Warnack[8] published the most extensive work on turbulent boundary layers exposed to favorable pressure gradients in nearly twenty years. There work was conducted at initial Reynolds numbers of $\mathrm{Re}_\theta = 862$ and 2564 for $K \leq 4.0 \times 10^{-6}$. A literature search has found that nearly all previous studies were conducted at initial Reynolds numbers of $\mathrm{Re}_\theta \ll 3000$[1]. Thus this new facility will permit us to investigate the response of the turbulent boundary layer to favorable pressure gradients at much larger initial Reynolds numbers and greater flow acceleration than previously explored.

Although larger initial Reynolds numbers are useful and needed, the true novelty of this experiment lies in the continuing use of a constant K region. Previous studies have relied upon a variable K region that peaked at a given value. This new facility will maintain a constant K region for a significant duration and makes for a clean experiment.

5.3 FTF-II Flight Testing

At present, there is insufficient tools available to immediately proceed with the continued development of a FTF-II flight experiment. The current experimental evidence suggests that K is not a reliable indicator of relaminarization. Further more, our ability to detect relaminarization has, at best, been shown in ground testing to be severely limited at present. Before a suitable FTF-II flight test design is completed and flown, several questions must be addressed, chief among these are:

1. Under what conditions will relaminarization occur and what is the governing parameter?
2. When relaminarization is present, what is the appropriate tool necessary to detect relaminarization?

The planned wind tunnel testing in the Hessert Center's 1.5 m $\times$ 1.5 m (5 ft $\times$ 5 ft) atmospheric wind tunnel is designed to answer these questions. Upcoming tests in the atmospheric wind tunnel will shed light on the nature of relaminarization and, it is believed, lead to the development of a new governing parameter. Once this is determined, the FTF-II design discussed previously may then be appropriately modified, so as to ensure relaminarization on the FTF-II in flight testing.

Based on the experimental evidence to date, it is believed that turbulent burst-sweep measurements will be a viable detection criterion for determining when and where relaminarization occurs. Development of this diagnostic tool will continue in wind tunnel tests with the ultimate goal being to use flush mounted hot film arrays in flight testing and then applying a burst-sweep event detector algorithm to the data to determine, either in real-time or post-flight, the location and nature of relaminarization at Mach and Reynolds numbers more typical of commercial high-lift systems.

[1]Only one case was found with a greater initial Reynolds number; Patel and Head[5] in 1968 investigated flow in a pipe with $\mathrm{Re}_\theta = 5900$.

6 Summary

Turbulent boundary layer relaminarization has been shown to potentially exist on high-lift systems from the results of van Dam, et al.[2] and a possible mechanism by which relaminarization may manifest itself has been illustrated. Under the current research effort supported by the NASA Dryden Flight Research Center, ground testing facilities have been developed at the University of Notre Dame in order to further our understanding of turbulent boundary layer relaminarization and to assess the importance of relaminarization in high-lift systems. To date, testing has been conducted in the 0.6 m $\times$ 0.6 m (2 ft $\times$ 2 ft) subsonic indraft wind tunnel at the Hessert Center for a range of constant acceleration parameters. Results (shape factor evolution, skin friction evolution, maximum turbulent intensity evolution, log-law behavior, etc...) are consistent with the presence of relaminarization in the expected cases; although there is some question as to whether these are adequate discriminators for determining the presence of relaminarization. In addition, a preliminary concepts for an in-flight relaminarization experiment on the FTF-II has been explored.

Experimental evidence suggests that the acceleration parameter, K, is not a viable parameter for determining the onset of relaminarization. This poses a large problem for designing a successful relaminarization flight test experiment, since there exists no definitive analysis tools to determine in advance when and where relaminarization would occur. However, preliminary evidence supports the claim that the turbulent bursting rate may be a direct indicator of relaminarization.

Future work will focus on the development of a new relaminarization facility in the University of Notre Dame's Hessert Center's atmospheric wind tunnel, which will provide a clean experiment for the further study of relaminarization. It is intended to use this facility to further assess the viability of the acceleration parameter and to develop a new relaminarization parameter to aid in the development of the proposed FTF-II flight test experiment. In addition, development will continue on the use of the turbulent burst-sweep event as a method for detecting turbulent boundary layer relaminarization and applying a detector algorithm to flush mounted hot films in order to construct an in-flight relaminarization detection tool. This work will culminate in an in-flight relaminarization experiment for the FTF-II and the suitable flow diagnostic tools to detect relaminarization in flight.

7 Bibliography

References

[1] F. O. Thomas, R. C. Nelson, and D. Fisher. Key topics for high-lift research: A joint wind tunnel/flight test approach. Technical report, NASA-Ames University Consortium, Joint Research Interchange, 1996.

[2] C. P. van Dam, P. M. H. W. Vijgen, L. P. Yip, and R. C. Potter. Leading-edge transition and relaminarization phenomena on a subsonic high-lift system. *AIAA*, Paper No. 93–3140, 1993.

[3] B.E. Launder. Laminarization of the turbulent boundary layer by acceleration. Technical Report 77, MIT Gas Turbine Lab, 1964.

[4] D.G. Wilson. Convective heat transfer to gas turbine blades. *Proc. Inst. Mech. Engrs.*, 1954.

[5] V.C. Patel and M.R. Head. Reversion of turbulent to laminar flow. *Journal of Fluid Mechanics*, 34:371–392, 1968.

[6] R. Narasimha and K.R. Sreenivasan. Relaminarization in highly accelerated turbulent boundary layers. *Journal of Fluid Mechanics*, 61:417–447, 1973.

[7] D. Warnack and H.F. Fernholz. The effects of a favorable pressure gradient and of the reynolds number on an incompressible axisymmetric turbulent boundary layer, part 1: The boundary layer. *Journal of Fluid Mechanics*, 359:329–356, 1998.

[8] D. Warnack and H.F. Fernholz. The effects of a favorable pressure gradient and of the reynolds number on an incompressible axisymmetric turbulent boundary layer, part 2: The boundary layer with relaminarization. *Journal of Fluid Mechanics*, 359:357–381, 1998.

[9] M. Ichimiya, I. Nakamura, and S. Yamashita. Properties of a relaminarizing turbulent boundary layer under a favorable pressure gradient. *Experimental Thermal and Fluid Sciences*, 17:37, 1998.

[10] K.R. Sreenivasan. Laminarescent, relaminarizing, and retransitional flows. *Acta Mechanica*, 44:1–48, 1982.

[11] M.A. Badri Narayanan and V. Ramjee. On the criteria for reverse transition in a 2-d boundary layer flow. *Journal of Fluid Mechanics*, 35:225–241, 1969.

[12] R. Narasimha and K.R. Sreenivasan. Relaminarization of fluid flows. *Advances in Applied Mechanics*, 19:221–309, 1979.

[13] H. Fiedler and M.R. Head. Intermittentcy measurements in the turbulent bounndary layer. *Journal of Fluid Mechanics*, 25:719, 1966.

[14] R.F. Blackwelder and L.S.G. Kovasznay. Large–scale motion of a turbulent boundary layer during relaminarization. *Journal of Fluid Mechanics*, 53:61–83, 1972.

[15] S.J. Kline, W.C. Reynolds, F.A. Schraub, and P.W. Runstadler. The structure of turbulent boundary layers. *Journal of Fluid Mechanics*, 30:741–773, 1967.

[16] P.S. Klebanoff. Characteristics of turbulence in a boundary layer with zero pressure gradient. Technical Report 3178, NACA, 1955.